Solid-State ^{23}Na and ^{27}Al MAS NMR Study of the Dehydration of $Na_2O \cdot Al_2O_3 \cdot 3H_2O$

Steven F. Dec,[†] Gary E. Maciel,*[,†] and John J. Fitzgerald*[,‡]

Contribution from the Departments of Chemistry, Colorado State University, Fort Collins, Colorado 80523, and South Dakota State University, Brookings, South Dakota 57007.
Received January 11, 1990

Abstract: The dehydration of $Na_2O \cdot Al_2O_3 \cdot 3H_2O$ was investigated as a function of dehydration temperature (100–600 °C) and dehydration time, using solid-state ^{23}Na and ^{27}Al nuclear magnetic resonance with high-speed magic-angle spinning (MAS). ^{23}Na and ^{27}Al MAS NMR spectra were recorded at field strengths of 8.4, 11.7, and 14.0 T. The field dependence of the NMR measurements aid in determining the presence of a number of chemically distinct sodium and aluminum sites. The MAS NMR results indicate that both untreated and dehydrated $Na_2O \cdot Al_2O_3 \cdot 3H_2O$ contain three chemically distinct sodium sites and one aluminum site. Simulation of the observed ^{23}Na and ^{27}Al spectra yields quadrupole coupling constants and asymmetry parameters for each sodium and aluminum site which, when used in combination with isotropic chemical shift measurements, permit various structures to be assigned to the sodium and aluminum sites. Water weight-loss measurements indicate that all structural changes observed in both the ^{23}Na and ^{27}Al NMR spectra are related to the progress of dehydration, although not all the water is removed, even after heating at 598 °C for extended times. For untreated $Na_2O \cdot Al_2O_3 \cdot 3H_2O$, the two major types of sodium sites are assigned to pseudooctahedral structures, while the aluminum site is assigned to a four-coordinate aluminum and the local chemical environment, $AlO_2(OAl)_2$, i.e., with two coordinating oxygen atoms that are bonded to other aluminum atoms and two that are not. For dehydrated $Na_2O \cdot Al_2O_3 \cdot 3H_2O$, the major sodium site is assigned to a pseudo-trigonal-bipyramidal structure, while the aluminum site is assigned to the tetrahedral AlO_4 environment. Minor sodium ion components in both hydrated and dehydrated $Na_2O \cdot Al_2O_3 \cdot 3H_2O$ may exist in zones of irregular, partially dehydrated sites of the sodium oxide type. A bulk chemical structural model of untreated $Na_2O \cdot Al_2O_3 \cdot 3H_2O$ consistent with these structural assignments is one in which aluminum atoms are covalently linked together via oxygen bridges to form rings or polymer chains. A bulk structural model of dehydrated $Na_2O \cdot Al_2O_3 \cdot 3H_2O$ that is proposed is based on monomeric AlO_4 tetrahedra linked by uniformly distributed five-coordinate sodium ions. This bulk structure differs from that of the stable forms of dehydrated sodium aluminate, established by X-ray diffraction, in which both sodium and aluminum ions are tetrahedrally coordinated, indicating that $NaAlO_2$ cannot be formed directly by dehydration of $Na_2O \cdot Al_2O_3 \cdot 3H_2O$ with use of the dehydration temperatures of this study.

Introduction

Multinuclear NMR studies of inorganic solids can potentially yield structural information based on nuclides of a number of different elements, an approach that overcomes some of the limitations of strategies based on data obtained from NMR studies of a single nuclide. For example, both ^{27}Al and ^{29}Si magic-angle spinning (MAS) NMR spectra are commonly obtained in structural studies of aluminosilicates and zeolites.[1-8] Klinowski et al.[4] have postulated, based on the apparent discrepancy measured for the amount of non-framework aluminum from ^{27}Al and ^{29}Si NMR spectra in calcined NH_4–Na–Y zeolite, that the unobserved aluminum in some of their ^{27}Al MAS NMR spectra is associated with aluminum species with very large quadrupole coupling constants. For a sample of H–rho zeolite, Vega and Luz[1] have suggested as one possibility for explaining the combination of both the ^{27}Al and ^{29}Si NMR results that the observed octahedral-aluminum dealumination product is connected to the zeolite framework, an interpretation that would be less convincing if there were no ^{29}Si NMR data.

A multinuclear NMR approach to the characterization of aluminum oxide and hydroxide systems has generally not been feasible. High-resolution solid-state ^1H NMR is not generally a routine technique,[9-13] and only recently has solid-state ^{17}O NMR been shown to be a useful method for the study of these solids.[14-16] To date, only ^{27}Al NMR has been used to any great extent to study Al–O and Al–O–H systems.[17-19]

For aluminates, the counterion (cation) is often based on a quadrupolar nucleus with $I = n/2$, where n is an odd integer greater than 1. While ^{27}Al NMR spectra were recorded for various aluminates[17] in some of the earliest high-resolution solid-state ^{27}Al MAS NMR studies, no systematic solid-state NMR study of countercations in the aluminate systems has been reported. In view of the role that these cations play in a diverse range of ceramic materials,[20-28] studies of these nuclei by high-resolution solid-state NMR techniques are expected to be of substantial

* Authors to whom correspondence should be addressed.
† Colorado State University.
‡ South Dakota State University.

(1) Vega, A. J.; Luz, Z. *J. Phys. Chem.* **1987**, *91*, 365-373.
(2) Luz, Z.; Vega, A. J. *J. Phys. Chem.* **1987**, *91*, 374-382.
(3) Fyfe, C. A.; Gobbi, G. C.; Kennedy, G. J. *J. Phys. Chem.* **1984**, *88*, 3248-3253.
(4) Klinowski, J.; Fyfe, C. A.; Gobbi, G. C. *J. Chem. Soc., Faraday Trans. 1* **1985**, *81*, 3003-3019.
(5) Pfeifer, H.; Freude, D.; Hunger, M. *Zeolites* **1985**, *5*, 274-286.
(6) Klinowski, J. *Prog. NMR Spectrosc.* **1984**, *16*, 237-309.
(7) Fitzgerald, J. J.; Hamza, A. I.; Bronnimann, C. E.; Dec, S. F. *Solid State Ionics* **1989**, *32/33*, 378-388.
(8) Alma, N. C. M.; Hays, G. R.; Samoson, A. V.; Lippmaa, E. T. *Anal. Chem.* **1984**, *56*, 729-733.
(9) Rosenberger, H.; Ernst, H.; Scheler, G.; Juenger, I.; Sonnenberger, R. *Z. Phys. Chem.* **1982**, *263*, 846-848.
(10) Rosenberger, H.; Scheler, G.; Buerger, H.; Jakob, M. *Colloids Surf.* **1984**, *12*, 53-58.
(11) Gerstein, B. C.; Chow, C.; Pembleton, R. G.; Wilson, R. C. *J. Phys. Chem.* **1977**, *81*, 565-570.
(12) Bronnimann, C. E.; Zeigler, R. C.; Maciel, G. E. *J. Am. Chem. Soc.* **1988**, *110*, 2023-2026.
(13) Bronnimann, C. E.; Hawkins, B. L.; Zhang, M.; Maciel, G. E. *Anal. Chem.* **1988**, *60*, 1743-1750.
(14) Schramm, S.; Oldfield, E. *J. Am. Chem. Soc.* **1984**, *106*, 2502-2506.
(15) Timken, H. K. C.; Schramm, S. E.; Kirkpatrick, R. J.; Oldfield, E. *J. Phys. Chem.* **1987**, *91*, 1054-1058.
(16) Walter, T. H.; Turner, G. L.; Oldfield, E. *J. Magn. Reson.* **1988**, *76*, 106-120.
(17) Muller, D.; Gessner, W.; Behrens, H.-J.; Scheler, G. *Chem. Phys. Lett.* **1981**, *79*, 59-62.
(18) Kunwar, A. C.; Thompson, A. R.; Gutowsky, H. S.; Oldfield, E. *J. Magn. Reson.* **1984**, *60*, 467-472.
(19) Fitzgerald, J. J. In *Antiperspirants and Deodorants*; Laden, K., Felger, C. B., Eds.; Marcel Dekker: New York, 1983; pp 119-292.
(20) Kingery, W. D.; Bowen, K. H.; Wholman, D. R. *Introduction to Ceramics*, 2nd ed.; John Wiley and Sons: New York, 1975.
(21) Ichinose, N. *Introduction to Fine Ceramics*; John Wiley and Sons: New York, 1987.
(22) *Ceramic Powder Science*; Messing, G. L., Mazdiyasni, K. S., Caurley, J. W., Haber, R. A., Eds.; American Ceramic Society: Westerville, OH, 1987.
(23) *Ceramic Materials for Electronics*; Buchanan, R., Ed.; Marcel Dekker: New York, 1986.

0002-7863/90/1512-9069$02.50/0

importance. The lack of widespread NMR study via half-integer quadrupolar nuclei is probably due to the following two factors: (1) The second-order quadrupolar frequency shift of the central ($^1/_2 \leftrightarrow -^1/_2$) transition of an odd-$n/2$ quadrupolar nucleus is not completely averaged to zero by MAS; and (2) this interaction can be very large, providing only highly "irregular" spectra at low magnetic fields. Recently, very high static magnetic fields have become available to alleviate this latter problem. In this work, it is shown for the case of ^{23}Na MAS NMR at a static field of 14.0 T that it is possible to observe both the major and minor sodium components present in $Na_2O{\cdot}Al_2O_3{\cdot}3H_2O$ and its dehydration products.

Sodium aluminate has extensive commercial utility as a source of aluminate ion and as a coagulating agent. Commercial grades of the material generally contain water of hydration;[29] a structural alteration accompanies the partial or complete removal of water. The dehydrated forms of sodium aluminate have been extensively studied with X-ray methods.[30] No X-ray data are available for the hydrated form, presumably because suitable crystals cannot be obtained. Thus, high-resolution solid-state NMR studies should provide valuable information regarding the structure of this commercially important material.

The dehydrated form, $NaAlO_2$, has been found to exist in two stable forms.[30] The β-$NaAlO_2$ form is stable at temperatures up to 470 °C, at which it transforms reversibly to the γ-$NaAlO_2$ form, which decomposes at temperatures greater than 1000 °C.[31] In the thermal studies reported herein, covering a temperature range of 100–600 °C, any measurable mass loss occurring during heating is due to loss of water only. The structural changes in these materials inferred from ^{23}Na and ^{27}Al MAS NMR spectra are therefore due to changes in the numbers and types of ligands coordinated to sodium and aluminum.

In this work we report high-resolution solid-state ^{23}Na and ^{27}Al MAS NMR results obtained on a series of $Na_2O{\cdot}Al_2O_3{\cdot}3H_2O$ samples that have been thermally treated at various temperatures as a function of time. Spectra for all samples were recorded with use of an external field of 14.0 T (600 MHz for ^{1}H). In addition, spectra of some samples were also obtained at 8.4 and 11.7 T. High-speed MAS techniques were used in order to effectively average dipolar and chemical shift anisotropy effects. ^{27}Al MAS NMR spectra were obtained as a function of field for the basic dimeric salt, $K_2Al_2O(OH)_6$, to aid in the structural assignments for aluminum in the sodium aluminate system. ^{23}Na MAS NMR spectra were also recorded on a series of model sodium salts in order to aid the structural assignment of the sodium cation sites in $Na_2O{\cdot}Al_2O_3{\cdot}3H_2O$ and its dehydration products.

Theoretical Background

The Hamiltonian, $\mathcal{H}$, for a system of quadrupolar nuclei can be written

$$\mathcal{H} = \mathcal{H}_Z + \mathcal{H}_D + \mathcal{H}_{CS} + \mathcal{H}_Q \qquad (1)$$

where $\mathcal{H}_Z$, $\mathcal{H}_D$, $\mathcal{H}_{CS}$, and $\mathcal{H}_Q$ are the Zeeman, dipolar, chemical shift, and quadrupolar Hamiltonians, respectively. Under magic-angle spinning conditions in which the rotational frequency of the sample is large compared to both $\mathcal{H}_D$ and $\mathcal{H}_{CS}$, but small compared to $\mathcal{H}_Q$, the observed resonance frequency is perturbed by $\mathcal{H}_Q$. In the high-field case, the frequency, ν, of the central ($^1/_2 \leftrightarrow -^1/_2$) transition of a non-integer quadrupolar nucleus is given for a rotating sample by[32]

$$\nu = \nu_0 + \left(\frac{3e^2qQ}{2I(2I-1)h}\right)^2\left(\frac{I(I+1)-\frac{3}{4}}{9\nu_0}\right)f(\eta,\Omega) \qquad (2)$$

where ν_0 is the Larmor frequency, e^2qQ/h is the quadrupole coupling constant (qcc), eq = V_{ZZ} is the ZZ component of the electric field gradient tensor, and I is the nuclear spin. The function $f(\eta,\Omega)$ is a complex function of the asymmetry parameter $\eta = (V_{XX} - V_{YY})/V_{ZZ}$ and angles Ω that relate the principal axis system of the electric field gradient tensor (X, Y, Z) to the laboratory frame. Equation 2 predicts that as the external field strength increases the second-order quadrupolar frequency shift decreases, i.e., the second term on the right-hand side of eq 2 becomes smaller. Thus, simpler and more highly resolved spectra should be obtained at higher field for non-integer quadrupolar nuclei.

The quadrupole coupling constant and asymmetry parameter depend on the distribution of charge about the nucleus of interest and can be used to extract structural information about the chemical environment of the nucleus. While ab initio techniques have been used to calculate the electric field gradient tensor components for a number of isolated molecules,[33,34] the application of such methods to complex solids such as $Na_2O{\cdot}Al_2O_3{\cdot}3H_2O$ may not be warranted at this time due to the large number of atoms involved. Less vigorous theoretical approaches may in some cases yield useful information about the types of ligands coordinated to a cation nucleus of interest. Such a theory has been developed for Mössbauer spectroscopy and applied to interpret Mössbauer spectra in terms of the number and types of ligands bound to the Mössbauer-observable cation atom.[35-37]

Experimental Section

Materials and Sample Preparation. Reagent grade sodium aluminate ($Na_2O{\cdot}Al_2O_3{\cdot}3H_2O$) was purchased from Fisher Scientific. About 1 g of a freshly ground sample was placed in an oven at the dehydration temperature noted herein as T_d. Independent temperature measurements showed that the samples reached thermal equilibrium in about 10 min for the temperature range studied. The accuracy of the temperature measurement is about ±2 °C. After the appropriate time period, samples were removed from the oven, quenched to room temperature, and stored in a desiccator prior to use. Samples were weighed both before and after dehydration. The dehydration mass loss is given in Table I.

The salt $K_2Al_2O(OH)_6$ was synthesized according to literature methods.[38] The model sodium salts, Na_2S, NaOH, NaF, NaCl, NaBr, and NaI, were reagent grade samples and were used as received without further purification.

NMR Measurements. ^{23}Na and ^{27}Al NMR spectra were recorded on a modified Nicolet NT-360 NMR spectrometer and on Bruker AM-500 and AM-600 NMR spectrometers, using home-built probes. To ensure minimum error in the quantitation of the observed NMR peak intensities, short excitation pulses (in most cases less than 22° tip angles) were used for the NMR measurements described below.[39] To assess the degree of quantitation, experiments were carried out on series of known α-$Al_2O_3/Na_2O{\cdot}Al_2O_3{\cdot}3H_2O$ mixtures and α-$Al_2O_3/KAl(SO_4)_2{\cdot}12H_2O$ mixtures; ^{27}Al NMR intensities were all within 15% of gravimetric predictions (much better for most samples). MAS speeds of 11.0–11.5 kHz were obtained with use of 6.0 mm (outer diameter) Torlon spinners on the NT-360 spectrometer. MAS speeds of 16–17 kHz were obtained with use of 4.5 mm (outer diameter) Torlon spinners on the AM-500 and

(24) *Better Ceramics Through Chemistry*; Brinker, C. J., Clark, D. E., Ulrich, D. R., Eds.; Mater. Res. Soc. Symp. Proc. No. 32; Elsevier: New York, 1984.
(25) *Ultrastructure Processing of Ceramics, Glasses, and Composites*; Hench, L. L., Ulrich, D. R., Eds.; Wiley-Interscience: New York, 1984.
(26) *Boron in Glass and Glass Ceramics*; Pye, L. D., Frechette, V. D., Kreidl, J. J., Eds.; Materials Science Research; Plenum Press: New York, 1978; Vol. 12.
(27) Lea, F. M. *The Chemistry of Cement and Concrete*, 2nd ed.; Edward Arnold: London, 1970.
(28) Soroka, I. *Portland Cement Paste and Concrete*; Chemical Publishing Co., Inc.: New York, 1980.
(29) Matthews, T. In *Speciality Inorganic Chemicals*; Thompson, R., Ed.; The Royal Society of Chemistry, Burlington House: London, 1981; pp 1–24.
(30) Thery, J.; Briancon, D.; Collongues, R. *Compt. Rend.* **1961**, *252*, 1475–1477.
(31) Wefers, K.; Misra, C. *Oxides and Hydroxides of Aluminum*, Alcoa Technical Paper No. 19, Revised; Alcoa Laboratories, 1987.
(32) Ganapathy, S.; Schramm, S.; Oldfield, E. *J. Chem. Phys.* **1982**, *77*, 4360–4365.
(33) Snyder, L. C. *J. Chem. Phys.* **1978**, *68*, 291–294.
(34) Asdjodi, M. R.; Gregory, R. V.; Lickfield, G. C.; Spencer, H. G.; Huffman, J. W.; Savitsky, G. B. *J. Chem. Phys.* **1987**, *86*, 1653–1656.
(35) Bancroft, G. M.; Platt, R. H. *Adv. Inorg. Chem. Radiochem.* **1972**, *15*, 59–258.
(36) Bancroft, G. M. *Mössbauer Spectroscopy*; John Wiley and Sons: New York, 1973.
(37) Parish, R. V. In *Mössbauer Spectroscopy Applied to Inorganic Chemistry*; Long, G. J., Ed.; Plenum Press: New York, 1988; Vol. 1, Chapter 16.
(38) Johansson, G. *Acta Chem. Scand.* **1966**, *20*, 505–515.
(39) Samoson, A.; Lippmaa, E. *Phys. Rev. B* **1983**, *28*, 6567–6570.

Table I. Weight Loss[a] and ^{23}Na and ^{27}Al Relative NMR Intensities[b] of $Na_2O{\cdot}Al_2O_3{\cdot}3H_2O$ and Its Dehydration Products

T_d, °C	time, min	mass loss, %	I_A	I_B	I_C	I_D	I_E	I_F	I_G
	0	0.0	42	12	46	0	0	100	0
100	10	0.7	40	15	43	0	2	100	0
	100	0.9	38	14	40	4	3	97	3
	250	2.1	37	14	38	9	2	88	12
	1010	8.8	30	10	28	30	2	60	40
110	10	0.3	42	13	40	3	3	100	0
	100	2.5	36	18	38	5	4	94	6
	250	7.3	28	14	28	26	3	75	25
	1060	15.3	12	9	19	59	2	17	83
128	10	0.9	39	18	39	2	3	97	3
	100	3.1	37	16	37	7	3	84	16
	250	17.1	26	14	26	30	4	17	83
	880	20.0	6	9	0	77	8	14	86
151	10	4.1	37	17	37	4	4	93	7
	100	20.2	7	8	0	78	6	10	90
	260	21.0	6	10	0	75	9	0	100
	980	20.7	0	9	0	84	7	0	100
172	10	2.5	37	21	36	4	3	85	15
	100	20.5	0	12	0	82	6	0	100
	250	21.4	0	7	0	87	6	0	100
	1150	21.3	0	10	0	85	5	0	100
201	10	7.1	27	16	25	29	3	70	30
	100	23.0	0	8	0	88	4	0	100
	250	21.3	0	9	0	87	4	0	100
	760	21.4	0	10	0	85	5	0	100
303	10	21.5	0	12	0	82	6	0	100
	100	21.5	0	13	0	80	7	0	100
	250	22.0	0	12	0	82	6	0	100
	790	22.1	0	12	0	80	8	0	100
400	10	22.2	0	11	0	84	5	0	100
	100	22.3	0	14	0	79	7	0	100
	250	22.4	0	14	0	80	6	0	100
	880	22.2	0	14	0	81	6	0	100
498	10	22.5	0	10	0	86	4	0	100
	100	22.5	0	12	0	84	4	0	100
	250	23.8	0	13	0	82	4	0	100
	1030	22.9	0	11	0	83	6	0	100
598	10	25.0	0	13	0	82	5	0	100
	100	23.5	0	13	0	82	5	0	100
	250	23.6	0	11	0	83	6	0	100
	850	21.9	0	11	0	82	8	0	100

[a] Mass loss in percent of total initial mass of sample. [b] Relative intensity, I_i, in percent of total intensity. A, B, C, D, E, F, and G are defined in Figure 1.

AM-600 spectrometers. Chemical shift references (by sample substitution) were aqueous solutions of 1 M NaCl and 1 M $AlCl_3{\cdot}6H_2O$ for ^{23}Na and ^{27}Al NMR, respectively. The reference resonance lines for these solutions were assigned a chemical shift of 0.0 ppm. Higher chemical shifts correspond to larger resonance frequencies and lower shielding constants.

^{23}Na 90° pulses for 1 M NaCl(aq) were 8.5, 7.0, and 6.5 μs at 95.2, 132.3, and 158.7 MHz, respectively. ^{27}Al 90° pulses for 1 M $AlCl_3$(aq) were 8.5, 6.5, and 6.0 μs at 93.8, 130.3, and 156.4 MHz, respectively. Pulse lengths of 1.0, 0.5, and 0.5 μs were used for ^{23}Na spectral determinations at 95.2, 132.3, and 158.7 MHz, respectively. Pulse lengths of 1.0, 0.5, and 0.5 μs were used for obtaining ^{27}Al spectra at 93.8, 130.3, and 156.4 MHz, respectively. The ^{23}Na MAS spectra were recorded with use of 10-ms relaxation delays. ^{23}Na NMR spectra recorded for some of the sodium aluminate samples at 158.7 MHz with 25-ms delays gave the same relative peak intensities. The ^{27}Al MAS spectra were recorded with 50-ms relaxation delays. ^{27}Al NMR spectra recorded for some of the sodium aluminate samples at 156.4 MHz with 100-ms delays gave the same relative peak intensities. The relative integrated intensity of each peak, I_i, was obtained from integration of the spectra. Peak intensities are listed in Table I for the various samples.

Spectral Simulations. Simulations of various second-order quadrupole resonance patterns[32] were obtained on a Sun 3/260 computer with use of the FTNMR software package developed by Hare Research, Inc. The experimental NMR line shapes were simulated assuming that only second-order quadrupole effects contribute to the line shapes observed. Exponential line broadening of 150–200 Hz was applied. This degree of line broadening may correspond to contributions to the observed residual line widths from residual dipolar effects and inhomogeneous chemical shift broadening. Estimated qcc and η values are reported as averages of a number of optimal simulations based upon visual comparison of the simulations with the observed spectra. Error estimates are based on the range of qcc or η values over which the computer simulations seem optimal by visual comparison.

Results

^{23}Na and ^{27}Al NMR. $Na_2O{\cdot}Al_2O_3{\cdot}3H_2O$ System. Figure 1 shows 14.0 T ^{23}Na and ^{27}Al MAS NMR spectra obtained on samples of $Na_2O{\cdot}Al_2O_3{\cdot}3H_2O$ after dehydration at various temperatures as a function of reaction time. The results are summarized in Table I. The ^{23}Na NMR spectra exhibit five intensity maxima, labeled A–E, with three of these maxima (A–C) attributable to the untreated material. The peak D becomes observable after heating at 100 °C for 100 min. The observation of peak E is apparent only after heating at relatively high temperatures or after heating for long times at low temperatures. The ^{27}Al spectra show two NMR intensity maxima, labeled F and G, with peak G being observed after heating at 100 °C for only 100 min.

For dehydration at 100 °C (Figure 1a) a reaction time of 100 min is needed to observe measurable changes in both the ^{23}Na and ^{27}Al NMR spectra. These changes are more pronounced for increasing reaction times but are still not complete at a reaction time of 1000 min. Similar behaviors, but with correspondingly larger extents of transformation, are seen in the results obtained at the other temperatures. For the second highest temperature shown, 128 °C, both the ^{23}Na and the ^{27}Al spectra show that the transformation is still incomplete after 880 min. For dehydration at 151 °C (Figure 1d), the NMR spectra (especially ^{27}Al) indicate that the dehydration process is complete after 980 min. Spectra obtained for dehydration temperatures of 172 and 201 °C (not shown here) are similar to those observed for dehydration at 151 °C, except that the dehydration process is complete in at most 100 min. Spectra obtained for dehydration temperatures of 303,

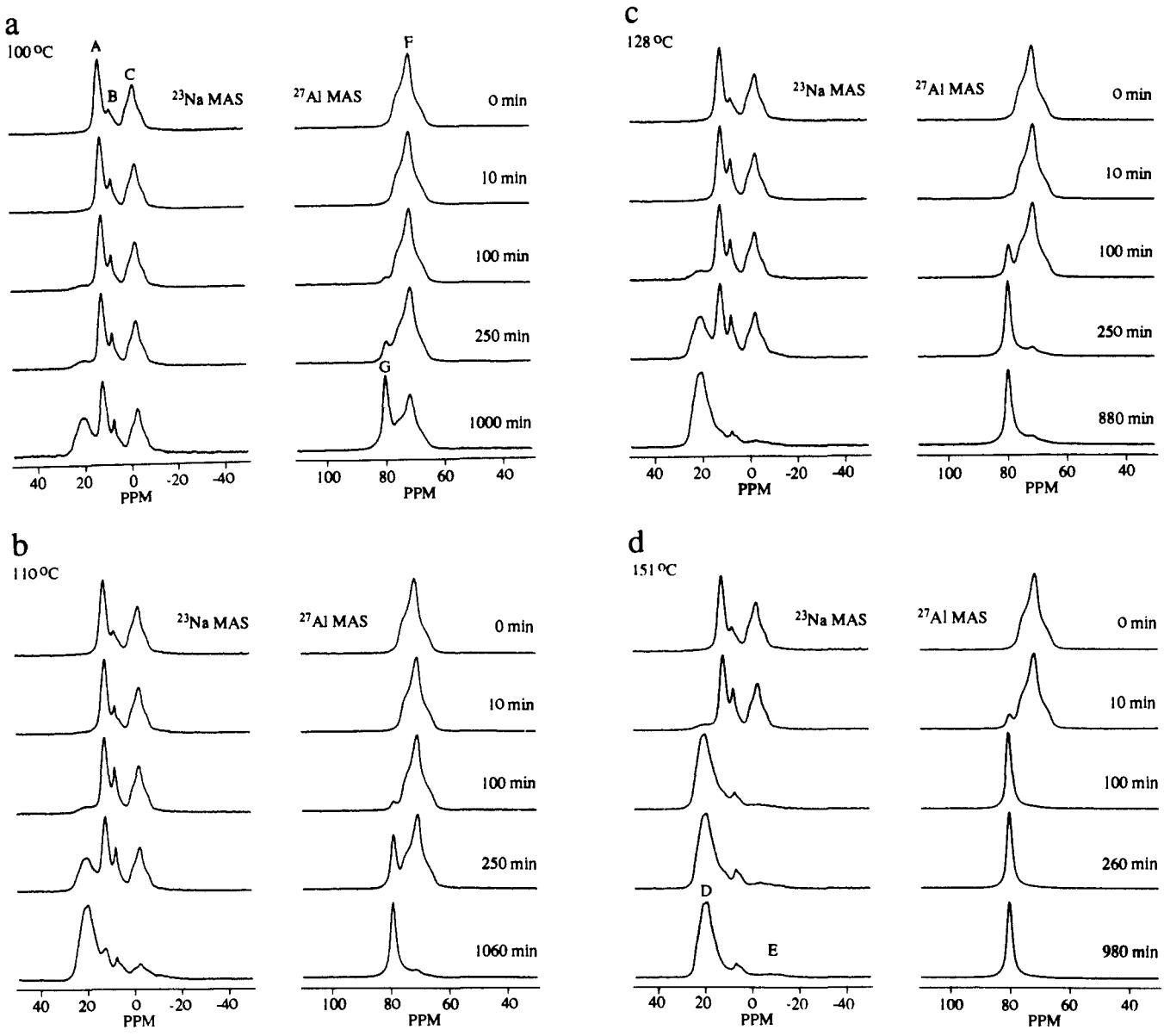

Figure 1. 14.0 T ^{23}Na and ^{27}Al MAS NMR spectra of $Na_2O{\cdot}Al_2O_3{\cdot}3H_2O$ as a function of dehydration temperature and time: (a) T_d = 100 °C; (b) T_d = 110 °C; (c) T_d = 128 °C; and (d) T_d = 151 °C.

400, 498, and 598 °C as a function of reaction time (not shown here) are similar to those observed for dehydration at 151 °C, except that the dehydration process is complete within 10 min.

Figure 1 shows that both ^{23}Na and ^{27}Al MAS NMR spectra of $Na_2O{\cdot}Al_2O_3{\cdot}3H_2O$ and its dehydration products contain resonances due to a number of chemically distinct sodium and aluminum sites. Variable magnetic field studies of the observed ^{23}Na and ^{27}Al NMR spectra of $Na_2O{\cdot}Al_2O_3{\cdot}3H_2O$ and its dehydration products, together with simulations of the observed spectra, enable one to examine these chemically different sodium and aluminum sites in more detail. In addition, the simulations permit the determination of the isotropic chemical shifts (δ) as well as qcc and η for each NMR resonance.[32]

The magnetic field dependence of the complex ^{27}Al MAS NMR line shape exhibited by the untreated $Na_2O{\cdot}Al_2O_3{\cdot}3H_2O$ (peak F of Figure 1) is shown in Figure 2a for 8.4, 11.7, and 14.0 T. The complex line shape of this resonance collapses and the intensity maximum shifts to higher frequency as the magnetic field is increased to 14.0 T, indicating that the dominant line-broadening mechanism is the second-order quadrupolar effect. This result is the type of behavior predicted by eq 2. Theoretical simulation of the observed 156.4-MHz ^{27}Al MAS NMR spectrum, based on eq 2, is shown in Figure 3a. This simulation yields a quadrupole coupling constant of 4.12 MHz, an asymmetry parameter of 0.85, and an isotropic chemical shift of 77.0 ppm. These parameters, together with those obtained for simulations of ^{27}Al NMR spectra obtained at 93.8 and 130.3 MHz, are summarized in Table II. The small differences in the qcc and η values obtained from simulations for the three different fields probably reflect the lack of inclusion of line width contributions due to chemical shift dispersion in the simulated line shapes.

For the dehydration product, the effect of magnetic field on the position and shape of the ^{27}Al NMR resonance (peak G of Figure 1) is shown in Figure 2b. The chemical shift corresponding to the intensity maximum of this tetrahedral aluminum atom is about 80 ppm and is independent of field; this value differs significantly from that (77 ppm) reported by Muller et al.[17] These authors did not correct the observed intensity maxima in their recorded spectra for the second-order quadrupolar frequency shift. The rather symmetrical line shape is observed to narrow as the external magnetic-field strength increases; this indicates that small, but non-negligible second-order quadrupolar effects are contributing to the observed line shapes.[40] Values of η cannot be determined from simulations of the observed spectra probably because chemical shift dispersion effects obscure the fine structure in the second-order quadrupolar powder pattern, i.e. the best fit quadrupole coupling constant value was found to reproduce the

(40) Samoson, A. *Chem. Phys. Lett.* **1985**, *119*, 29–32.

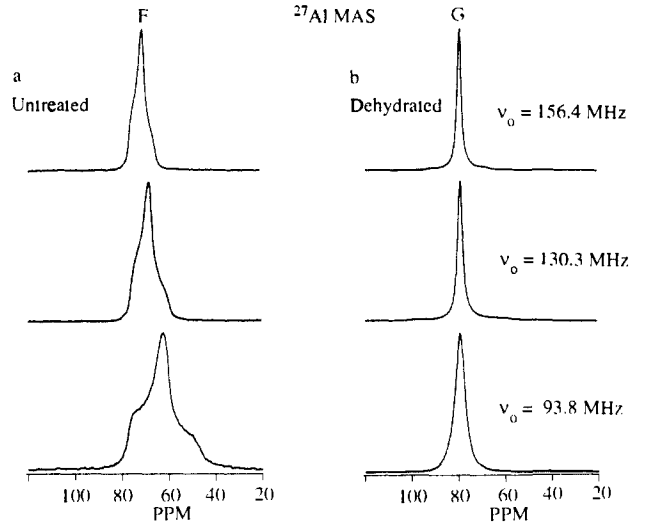

Figure 2. ^{27}Al MAS NMR spectra as a function of field: (a) untreated $Na_2O{\cdot}Al_2O_3{\cdot}3H_2O$—top, ν_0 = 156.4 MHz; middle, ν_0 = 130.3 MHz; bottom, ν_0 = 93.8 MHz; (b) dehydrated $Na_2O{\cdot}Al_2O_3{\cdot}3H_2O$—top, ν_0 = 156.4 MHz; middle, ν_0 = 130.3 MHz; botton ν_0 = 93.8 MHz.

observed spectra equally well for all possible values of η ($0 \leq \eta \leq 1$). Simulation of the spectrum at 156.4 MHz yields δ = 81.0 ppm and qcc = 2.0 MHz. Values of δ and qcc for the other two fields employed are similar and are given in Table II.

Figure 4a shows ^{23}Na MAS NMR spectra, obtained as a function of magnetic field, for untreated $Na_2O{\cdot}Al_2O_3{\cdot}3H_2O$. The ^{23}Na NMR peak B is well resolved only at 158.7 MHz (600-MHz spectrometer). For peaks A and C, the complex line shapes are seen to collapse and their intensity maxima shift to higher frequency with increasing field strength, indicating that the dominant line-broadening mechanism in both cases is the second-order quadrupolar effect. Simulation of the spectrum obtained at 158.7 MHz (excluding peak B) is shown in Figure 3b. Values of δ, qcc, and η obtained from simulations of spectra obtained at 95.2, 132.3, and 158.7 MHz are given in Table III. Since peak B is not observed at 95.2 MHz and is only partially resolved at 132.3 MHz, no inference can be made as to the cause of the residual line broadening observed for this particular peak. Thus, its isotropic chemical shift is arbitrarily taken as the position of the intensity maximum (ca. 8 ppm) and values of qcc and η are not reported.

Figure 4b shows ^{23}Na MAS NMR spectra obtained on the final dehydration product as a function of magnetic field. These results indicate that the intensity maxima at 20, 8, and −10 ppm are due to three chemically distinct sodium nuclei. The peak with an intensity maximum at 8 ppm, which is resolved at 158.7 MHz and appears as a shoulder at 132.3 MHz, is assigned to the ^{23}Na NMR peak B of the untreated material, based on comparison of its chemical shift with that of the untreated material. While peaks D and E are resolved at both 158.7 and 132.3 MHz, peak D completely dominates the spectrum recorded at 95.2 MHz, obscuring any other peaks. The complex line shape of peak D is seen to collapse and the position of its intensity maximum shifts to higher frequency at higher field, supporting the interpretation that the source of this line shape is the second-order quadrupolar effect. Values of δ, qcc, and η obtained from simulations of the ^{23}Na NMR spectra obtained at 95.2, 132.3, and 158.7 MHz are included in Table III. The broad peak E has a rather featureless line shape at 158.7 and 132.3 MHz and is not convincingly detected at 95.2 MHz. Its isotropic chemical shift is arbitrarily taken as the position of its apparent intensity maximum, and values of qcc and η are not reported.

Table II. ^{27}Al NMR Parameters of $Na_2O{\cdot}Al_2O_3{\cdot}3H_2O$ and Its Dehydration Product

peak	ν_0, MHz	δ, ppm	qcc, MHz	η
F	156.4	77.0	4.12 ± 0.06	0.85 ± 0.03
	130.3	76.4	4.11 ± 0.04	0.85 ± 0.03
	93.8	77.5	4.13 ± 0.03	0.89 ± 0.03
G[a]	156.4	81.0	2.0 ± 0.2	
	130.3	81.1	1.8 ± 0.1	
	93.8	82.1	1.8 ± 0.1	

[a] The values of the quadrupole coupling constant were found to fit equally well the observed line shapes for all possible values of η, i.e., $0 \leq \eta \leq 1$. The fine structure of the second-order quadrupole powder patterns is obscured, probably by chemical shift dispersion effects. Therefore, values of η cannot be determined and are not reported. The isotropic chemical shift was obtained by correcting the observed intensity maxima by the average of the second-order quadrupolar frequency shift determined from simulations for η = 0 and 1.

Table III. ^{23}Na NMR Parameters of $Na_2O{\cdot}Al_2O_3{\cdot}3H_2O$ and Its Dehydration Products

peak	ν_0, MHz	δ, ppm	qcc, MHz	η
A	158.7	14.2	1.3 ± 0.1	0.75 ± 0.05
	132.3	14.9	1.54 ± 0.08	0.75 ± 0.05
	95.2	13.4	1.26 ± 0.04	0.74 ± 0.04
B	158.7	7.7[a]		
	132.3	8.4[a]		
	95.2			
C	158.7	1.9	1.91 ± 0.04	0.76 ± 0.03
	132.3	1.8	1.90 ± 0.03	0.77 ± 0.03
	95.2	2.3	1.92 ± 0.04	0.75 ± 0.03
D	158.7	26.3	2.19 ± 0.03	0.65 ± 0.03
	132.3	25.7	2.18 ± 0.04	0.63 ± 0.03
	95.2	26.3	2.20 ± 0.03	0.59 ± 0.03
E	158.7	−10[a]		
	132.3	−10[a]		
	95.2			

[a] Apparent chemical shifts. Analysis for a second-order quadrupole effect was not carried out because of a poorly defined line shape.

^{27}Al NMR. $K_2Al_2O(OH)_6$ System. Figure 5 shows ^{27}Al MAS NMR spectra obtained at 156.4, 130.3, and 93.8 MHz. The magnetic field dependence of the observed complex line shape indicates that the dominant line-broadening effect is probably caused by second-order quadrupolar effects. Simulation of the 156.4-MHz spectrum yields δ = 81.3 ppm, qcc = 4.48 MHz, and

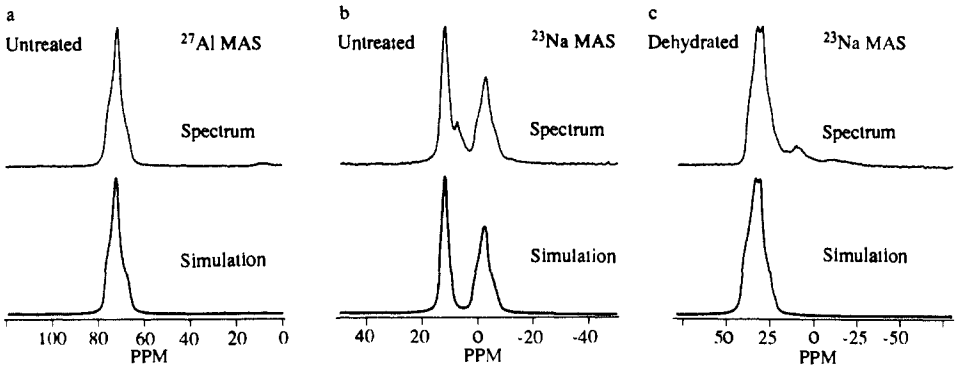

Figure 3. Observed and simulated 14 T ^{23}Na and ^{27}Al MAS spectra: (a) observed (top) and simulated (bottom) ^{27}Al MAS NMR spectra of untreated $Na_2O{\cdot}Al_2O_3{\cdot}3H_2O$; (b) observed (top) and simulated (bottom) ^{23}Na MAS NMR spectra of untreated $Na_2O{\cdot}Al_2O_3{\cdot}3H_2O$; (c) observed (top) and simulated (bottom) ^{23}Na MAS NMR spectra of dehydrated $Na_2O{\cdot}Al_2O_3{\cdot}3H_2O$.

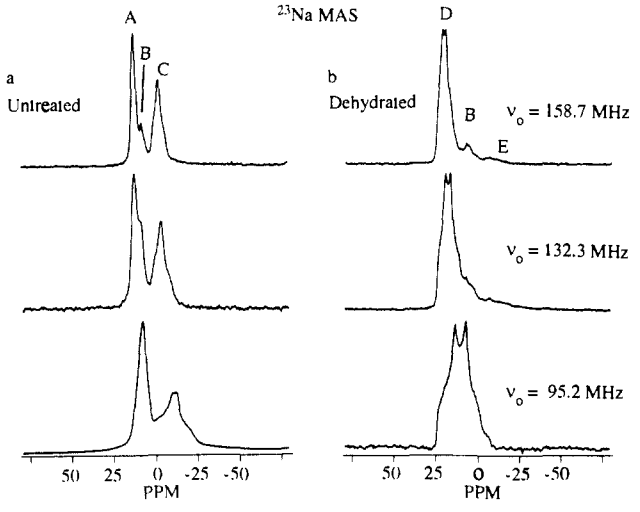

Figure 4. ^{23}Na MAS NMR spectra as a function of field: (a) untreated $Na_2O{\cdot}Al_2O_3{\cdot}3H_2O$—top, ν_0 = 158.7 MHz; middle, ν_0 = 132.3 MHz; bottom, ν_0 = 95.2 MHz; (b) dehydrated $Na_2O{\cdot}Al_2O_3{\cdot}3H_2O$—top, ν_0 = 158.7 MHz; middle, ν_0 = 132.3 MHz; botton ν_0 = 95.2 MHz.

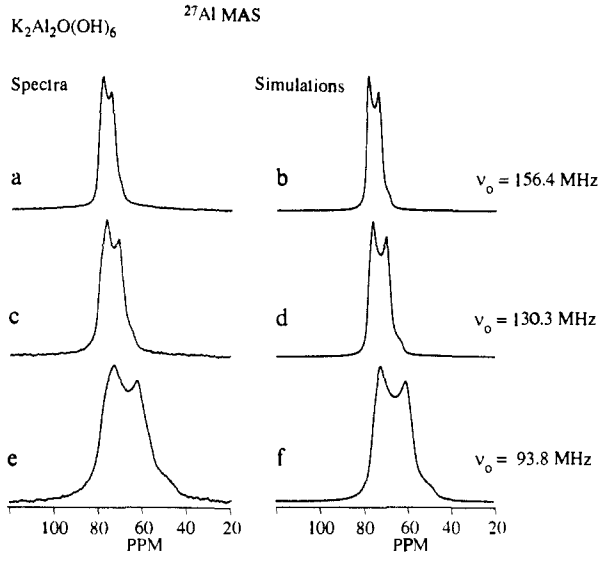

Figure 5. ^{27}Al MAS NMR spectra of $K_2Al_2O(OH)_6$ as a function of field: (a) spectrum recorded at 156.4 MHz; (b) simulation of spectrum a; (c) spectrum recorded at 130.3 MHz; (d) simulation of spectrum c; (c) spectrum recorded at 93.8 MHz; (f) simulation of spectrum e.

η = 0.19. Results obtained at the other two fields employed are similar and are included in Table IV along with ^{23}Na results on some model compounds.

^{23}Na NMR. Model Compound Studies. In order to assign the various peaks appearing in the ^{23}Na MAS NMR spectra, correlation of isotropic ^{23}Na chemical shifts with specific local sodium sites is necessary. While Ganapathy et al.,[32] Kundla et al.,[41] and Buhl et al.[42] have reported isotropic ^{23}Na chemical shift data on such compounds as sodium sulfate, sodium nitrite, and hydrosodalite, no systematic study of the relationship between sodium coordination and isotropic ^{23}Na chemical shifts has been reported. Hence, isotropic chemical shift measurements were made on model compounds in the hope of providing benchmarks for characterizing the coordination numbers of the various sodium sites present in the $Na_2O{\cdot}Al_2O_3{\cdot}3H_2O$ system.

Figure 6 shows 158.7-MHz ^{23}Na MAS NMR spectra of a number of model compounds, i.e., Na_2S, NaOH, NaF, NaCl, NaBr, and NaI. The sodium in Na_2S has a coordination number (CN) of four, with tetrahedral symmetry;[43] NaOH has CN = 5;[44] and the sodium halides have CN = 6, with octahedral symmetry.[43] The ^{23}Na NMR spectra of this series of compounds demonstrate that the solid-state NMR chemical shift range of ^{23}Na is on the order of 50 ppm, the same order of magnitude as that found in solid-state ^{27}Al NMR.[6] One sees that four-, five-, and six-coordinate sodium sites have isotropic chemical shifts of about 50, 21, and −3 to 7 ppm, respectively. However, because the number of model compounds that have been investigated to date is limited, this empirical approach is not yet definitive. The nature and extent of the overlap of the chemical shift ranges of, for example, five- and six-coordinate sodium ions is not well-known. The line width of the NaF resonance is noticably larger than that for the other sodium halides and is due to the larger heteronuclear dipolar interactions experienced by the ^{23}Na nuclei in NaF relative to the

Table IV. ^{23}Na and ^{27}Al NMR Parameters of Model Compounds

compd	ν_0, MHz	δ,[e] ppm	qcc, MHz	η
	^{23}Na NMR Parameters			
Na_2S[a]	158.7	49.7[e]		
	132.3	49.9[e]		
NaOH[b]	158.7	21.1	3.59 ± 0.03	0.07 ± 0.02
	132.3	21.2	3.57 ± 0.04	0.07 ± 0.02
NaF[c]	158.7	7.2[e]		
	132.3	7.3[e]		
NaCl[c]	158.7	7.2[e]		
	132.3	7.3[e]		
NaBr[c]	158.7	5.1[e]		
	132.3	5.3[e]		
NaI[c]	158.7	−3.2[e]		
	132.3	−3.0[e]		
	^{27}Al NMR Parameters			
$K_2Al_2O(OH)_6$[d]	156.4	81.3	4.48 ± 0.04	0.19 ± 0.02
	130.3	81.2	4.46 ± 0.06	0.23 ± 0.02
	93.8	81.2	4.33 ± 0.06	0.21 ± 0.02

[a] Tetrahedral. [b] Coordination number 5. [c] Octahedral. [d] Coordination number 4. [e] Apparent chemical shifts. Analysis for a second-order quadrupole effect was not carried out because the intensity maxima and line widths of these resonance lines were independent of field within experimental error, indicating that quadrupolar effects are negligibly small.

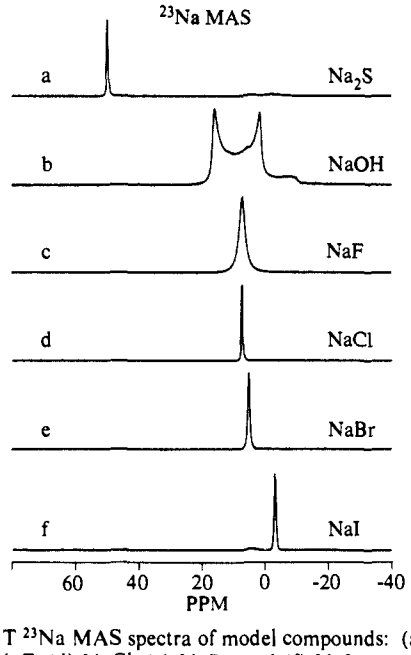

Figure 6. 14 T ^{23}Na MAS spectra of model compounds: (a) Na_2S, (b) NaOH, (c) NaF, (d) NaCl, (e) NaBr, and (f) NaI.

(41) Kundla, E.; Samoson, A.; Lippmaa, E. *Chem. Phys. Lett.* **1981**, *83*, 229–232.
(42) Buhl, J.-Ch.; Engelhardt, G.; Felsche, J.; Luger, S.; Foerster, H. *Ber. Bunsen-Ges. Phys. Chem.* **1988**, *92*, 176–181.
(43) Mahan, B. H. *University Chemistry*, 2nd ed.; Addison-Wesley: Reading, MA, 1969; p 115.
(44) Wells, A. F. *Structural Inorganic Chemistry*, 5th ed.; Clarendon Press: Oxford 1984; p 631.

other sodium halides. Only the ^{23}Na NMR spectrum of NaOH shows a complex line shape. This is expected because of its low symmetry.[44] Simulations (not shown here) of the ^{23}Na NMR spectra of NaOH obtained at 132.3 and 158.7 MHz yield a quadrupole coupling constant of 3.6 MHz, an asymmetry parameter of 0.07, and an isotropic chemical shift of 21 ppm. For the other model compounds, the position of the intensity maximum of each resonance line is taken as the isotropic chemical shift, since the line widths and the positions of the intensity maxima of these spectra are independent of field, indicating that quadrupolar effects are negligibly small.[32,40] The ^{23}Na NMR parameters of these model compounds are summarized in Table IV. These results are used to make tentative structural assignments of the resonance lines observed in the spectra of $Na_2O·Al_2O_3·3H_2O$ and its dehydration products.

Dehydration Kinetics. The resolution that can be obtained in ^{23}Na and ^{27}Al MAS NMR spectra obtained with a static magnetic field strength of 14.0 T permits the determination of integrated intensities for each peak present. On this basis, the kinetics of the dehydration of $Na_2O·Al_2O_3·3H_2O$ can be followed independently for each distinct sodium and aluminum site observed. In addition, gravimetric measurements of this process allow the ^{23}Na and ^{27}Al MAS NMR spectral changes to be correlated with the mass loss.

All of the observed mass loss during dehydration of $Na_2O·Al_2O_3·3H_2O$ at the temperatures used in this study is due to loss of water. Thus, the relative integrated intensities that are obtained from integration of the ^{23}Na and ^{27}Al MAS NMR spectra should accurately reflect the rate at which changes in coordination of the sodium and aluminum atoms occur during *dehydration* of $Na_2O·Al_2O_3·3H_2O$.

For a reaction that behaves empirically as a first-order (rate) process, the mole fraction of a reactant i at time t, $x_i(t)$, is given by

$$x_i(t) = x_{i0}e^{-kt} \tag{3}$$

where k is the rate constant governing the process and x_{i0} is the initial mole fraction of reactant i. For the reaction products, assuming no parallel reactions, the mole fraction at time t is given by

$$x_j(t) = x_{jm}(1 - e^{-kt}) \tag{4}$$

where x_{jm} is the maximum mole fraction of product j (corresponding to $t = \infty$). The number of moles of water removed by heating is calculated from the mass loss (Table I). The maximum number of moles of water lost per mole of untreated $Na_2O·Al_2O_3·3H_2O$ was determined from the average mass loss for all heating conditions for which the NMR spectra indicated that the reaction was complete. The result is $x_{H_2Om} = 0.897$. Since sodium and aluminum atoms are conserved during thermal dehydration of $Na_2O·Al_2O_3·3H_2O$, it is possible to determine the mole fraction of a particular sodium or aluminum site from the ^{23}Na and ^{27}Al NMR spectra. These are given by the relative intensities of the individual peaks, as the NMR spectra were obtained under conditions that avoid saturation/relaxation problems. Thus, in terms of the peaks identified in Figure 1, $x_{A0} = 0.421$, $x_{C0} = 0.460$, $x_{F0} = 1.000$, $x_{Dm} = 0.828$, and $x_{Gm} = 1.000$. The vaue of x_{Dm} was taken from the average of the relative intensities of peak D of all ^{23}Na NMR spectra for which the reaction was complete. The best fit of the kinetic data summarized in Table I was obtained by holding these values of x_{i0} and x_{im} fixed, using non-linear least-squares techniques.[45] Equations 3 and 4 do not adequately describe the rate data for dehydration temperatures greater than 151 °C, possibly because of additional dehydration processes at these high dehydration temperatures and perhaps because of the constraints of limited data points obtained over short dehydration time periods. Rate constants for the dehydration temperatures of 100, 110, 128, and 151 °C obtained in this manner are given in Table V. Plots of selected kinetic data are given in Figure 7. On the basis of comparison of the starting material's empirical formula, $Na_2O·Al_2O_3·3H_2O$, with the mass loss observed for the conditions used for a dehydration reaction that is considered complete on the basis of no further measurable change in the ^{23}Na and ^{27}Al NMR spectra, one can conclude that all of the water is not completely removed even after heating at 598 °C for 880 min. These data (Table I) show that only 2.7 mol of water are lost per mol of $Na_2O·Al_2O_3·3H_2O$ for long heating times at high dehydration temperatures.

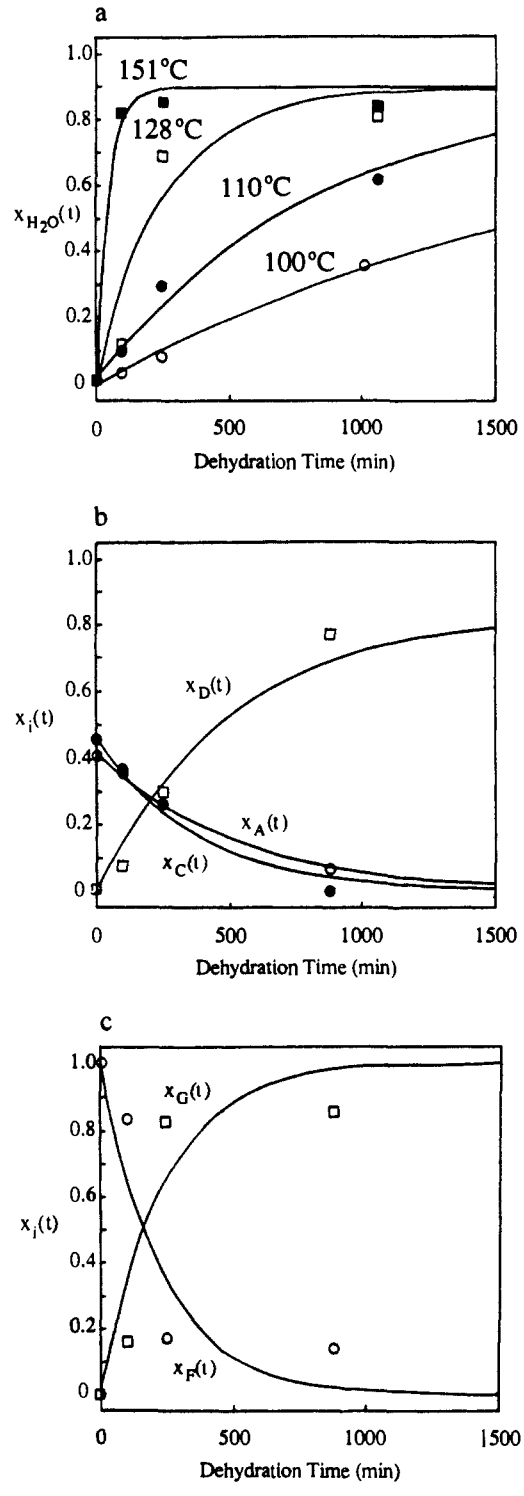

Figure 7. Plots of $x_i(t)$ versus dehydration time for water and peaks A, C, D, F, and G at selected dehydration temperatures: (a) $x_{H_2O}(t)$ versus dehydration time at T_d = 100 °C (○), T_d = 110 °C (●), T_d = 128 °C (□), and T_d = 151 °C (■); (b) $x_A(t)$ (○), $x_C(t)$ (●), and x_D (□) versus dehydration time at T_d = 128 °C; (c) $x_F(t)$ (○) and $x_G(t)$ (□) versus dehydration time T_d = 128 °C.

(45) Bevington, P. R. *Data Reduction and Error Analysis for the Physical Sciences*; McGraw-Hill Book Co.: New York, 1969.

Table V. Rate Constants, $k_i \times 10^4$ (min^{-1}), of Water Loss and Sodium and Aluminum Site Intensity Changes[a,b]

T_d, °C	k_{H_2O}	k_A	k_C	k_D	k_F	k_G
100	4.8 (0.3)	3.7 (0.6)	5.4 (0.8)	4.6 (0.1)	5.0 (0.2)	5.0 (0.2)
110	12 (1)	14 (1)	11 (3)	12 (1)	14 (2)	14 (2)
128	40 (10)	19 (2)	26 (5)	20 (3)	40 (10)	40 (10)
151	220 (30)	160 (30)	280 (40)	200 (60)	190 (30)	190 (30)

[a] Number in parentheses indicates estimated error in rate constant. [b] The rate constant k_{H_2O} describes the rate at which water is removed during dehydration (eq 4). The rate constants k_A, k_C, and k_F describe the decrease in the intensity of peaks A, C, and F, respectively (eq 3). The rate constants k_D and k_G describe the increase in the intensity of peaks D and G, respectively (eq 4).

Discussion

Analysis of the solid-state reaction kinetics, summarized in Figure 7, indicates that the major chemical transformations responsible for changes in the ^{23}Na and ^{27}Al MAS NMR spectra during the dehydration of $Na_2O{\cdot}Al_2O_3{\cdot}3H_2O$ are governed by a process with a rate similar to the rate of water loss. One sees from Table V that increases of the intensity of peak G in the ^{27}Al MAS NMR spectra occur with the same rate constant as the rate constant associated with the decrease of peak F; this is expected, because aluminum in the site associated with peak F is the only source of aluminum NMR intensity in untreated $Na_2O{\cdot}Al_2O_3{\cdot}3H_2O$.

Inspection of Table V also confirms the expectation that the increase in intensity of peak D occurs with a rate constant that is roughly the mean of the rate constants for the intensity decreases of peaks A and C; i.e., the number of sodiums in the peak D site increases at the combined rate at which the intensity of peaks A and C decreases during dehydration. Thus, the sodium sites assigned to peaks A and C in the ^{23}Na MAS NMR spectra are indeed both sources for the major sodium site, described by peak D, in the dehydration product.

^{27}Al NMR. Structural Assignments. Extensive solid-state ^{27}Al NMR data in the literature[6,17,19,46-50] indicate that the resonances of $Na_2O{\cdot}Al_2O_3{\cdot}3H_2O$ and its dehydration product (isotropic chemical shifts of about 77 and 81 ppm, respectively) are due to four-coordinate aluminums with four nearest-neighbor oxygen atoms. The small isotropic ^{27}Al chemical shift difference and the major change in the observed line shape between $Na_2O{\cdot}Al_2O_3{\cdot}3H_2O$ and its dehydration product are consistent with nearest-neighbor differences of aluminum sites in these two samples, i.e., differences in the moieties, X (if any), attached to oxygen in $Al(OX)_4$ structures.

The ^{27}Al NMR spectra of the model compound $K_2Al_2O(OH)_6$ in Figure 5 show the effect of next-nearest-neighbors on the observed line shape of the ^{27}Al NMR resonance in this sample. The measured asymmetry parameter, $\eta = 0.19$, is reasonably close to 0, which corresponds to a C_{3v} aluminum symmetry.[35,36] For $K_2Al_2O(OH)_6$, the local aluminum structure can be approximated by the C_{3v} $AlO_3(OAl)$ type structure (I), i.e., a structure in which only one X in the local formula $Al(OX)_4$ is aluminum, with three oxygens present as OH oxygens.

I II

The line shape of the ^{27}Al NMR resonance for untreated $Na_2O{\cdot}Al_2O_3{\cdot}3H_2O$ (Figure 2a) can also be rationalized on the basis of next-nearest-neighbor effects. The measured asymmetry parameter, $\eta = 0.85$, is very close to 1, which corresponds to a C_{2v} aluminum symmetry,[35,36] such as for aluminum with the local structure $AlO_2(OAl)_2$, structure II, with two oxygens present as OH oxygens. Thus, aluminum in untreated $Na_2O{\cdot}Al_2O_3{\cdot}3H_2O$ is here assigned the local structure $AlO_2(OAl)_2$.

The line shape of the ^{27}Al NMR resonance in dehydrated $Na_2O{\cdot}Al_2O_3{\cdot}3H_2O$ (Figure 2b) and the fact that increasing the field narrows the line somewhat show that second-order quadrupolar effects in this sample are significant but small. These results imply that the next-nearest-neighbors of aluminum in this sample are relatively symmetrically situated. The two types of local aluminum structures that are consistent with these ^{27}Al NMR results for this system are AlO_4 and $Al(OAl)_4$. The structure $Al(OAl)_4$ is not likely, since the isotropic ^{27}Al chemical shift of aluminum in such a structure is 63 ppm.[18] This value is nearly 20 ppm to higher shielding than what is observed for the isotropic ^{27}Al chemical shift in the dehydrated form of $Na_2O{\cdot}Al_2O_3{\cdot}3H_2O$. Thus, aluminum in dehydrated $Na_2O{\cdot}Al_2O_3{\cdot}3H_2O$ is assigned to the local structure AlO_4, in which each of the oxygens is ionic.

^{23}Na NMR. Structural Assignments. For untreated $Na_2O{\cdot}Al_2O_3{\cdot}3H_2O$, the field dependence of the ^{23}Na MAS NMR spectra indicates that peaks A, B, and C are due to three different sodium sites. Peaks B and C, with isotropic chemical shifts of about 8.0 and 2.0 ppm, respectively, are assigned to six-coordinate sodium ions on the basis of the chemical shift patterns stated above. Peak A, with an isotropic chemical shift of about 14 ppm, is also tentatively assigned to a sodium ion site with six ligands.

The major sodium ion components of untreated $Na_2O{\cdot}Al_2O_3{\cdot}3H_2O$, corresponding to peaks A and C, both have non-zero quadrupole coupling constants and $\eta = 0.75$. Thus, peaks A and C must correspond to highly distorted octahedral structures, since it is known[35,36] that ideal octahedra have $V_{XX} = V_{YY} = V_{ZZ} = 0$.

Peak E of the dehydration product, with an apparent isotropic chemical shift of about −10 ppm, is also tentatively assigned to sodium with a coordination number of six. The isotropic chemical shift of this sodium site lies slightly outside the range of chemical shifts observed for the octahedral sodium halides and may indicate that the coordination number of this sodium species is greater than six, although a second-order quadrupolar frequency shift cannot be ruled out. It should also be noted that peak E may actually be present in untreated $Na_2O{\cdot}Al_2O_3{\cdot}3H_2O$; because of its relatively low intensity and the partial overlap of this resonance line with peak C, it is possible that peak E cannot be resolved in the ^{23}Na NMR spectrum of untreated $Na_2O{\cdot}Al_2O_3{\cdot}3H_2O$.

The major sodium site of the dehydration product, represented by peak D, has an isotropic chemical shift of about 26 ppm and is assigned on the basis of the patterns stated above to sodium ion with a coordination number of five. The asymmetry parameter of about 0.6 indicates that this species does not have an ideal trigonal-bipyramidal structure, since $\eta = 0$ for such a structure.[35,36] Thus, peak D is assigned to sodium ions with a highly distorted trigonal-bipyramidal structure. This assignment differs from that determined from X-ray analysis[30] of β-$NaAlO_2$; the X-ray work shows that the sodium ions have a coordination number of four. Thus, our work shows that crystalline $NaAlO_2$ is not formed by dehydration of $Na_2O{\cdot}Al_2O_3{\cdot}3H_2O$ at the dehydration temperatures of this work (less than or equal to 600 °C).

Global Structures. The ^{23}Na and ^{27}Al MAS NMR spectra show that major structural changes occur when $Na_2O{\cdot}Al_2O_3{\cdot}3H_2O$ is thermally dehydrated. Untreated $Na_2O{\cdot}Al_2O_3{\cdot}3H_2O$ has only one type of aluminum site but two major sodium sites. A wide variety of global structures are consistent with the local aluminum

(46) Lippmaa, E.; Magi, M.; Samoson, A.; Tarmak, M.; Engelhardt, G. *J. Am. Chem. Soc.* **1981**, *103*, 4992-4996.
(47) Mueller, D.; Hoebbel, D.; Gessner, W. *Chem. Phys. Lett.* **1981**, *84*, 25-29.
(48) Muller, D.; Jahn, E.; Ladwig, G.; Haubenreisser, U. *Chem. Phys. Lett.* **1984**, *109*, 332-336.
(49) Kinsey, R. A.; Kirkpatrick, R. J.; Hower, J.; Smith, K. A.; Oldfield, E. *Am. Miner.* **1985**, *70*, 537-548.
(50) Kirkpatrick, R. J.; Smith, K. A.; Schramm, S.; Turner, G.; Yang, W. H. *Annu. Rev. Earth Planet. Sci.* **1985**, *13*, 29-47.

structure, $AlO_2(OAl)_2$, assigned above to untreated $Na_2O·Al_2O_3·3H_2O$. Both ring structures and linear chain structures are plausible for the aluminate moiety in untreated $Na_2O·Al_2O_3·3H_2O$, similar to those reported in aqueous and solid-state silicate[51-55] and solid-state aluminate[56,57] chemistry. The simplest cyclic oligomeric ring structure is a six-membered ring with three alternating aluminum and oxygen atoms (an aluminum trimer). An additional ring structure with $AlO_2(OAl)_2$ units could include a cyclic aluminum tetramer, analogous to the cyclic tetrameric $SiO_2(OSi)_2$-type silicate species identified by ^{29}Si NMR in sodium and potassium silicate solutions,[51,52,54,55] and its salt, $K_4H_4Si_4O_{12}$, which has been examined by solid-state ^{29}Si NMR.[53] Double-ring silicate structures, such as $[Si_6O_{15}]^{6-}$, $[Si_8O_{20}]^{8-}$, and $[Si_{10}O_{25}]^{10-}$ ions found in solution and solid-state silicate chemistry,[51-55] are not plausible models for the aluminates in untreated $Na_2O·Al_2O_3·3H_2O$, since the silicate species contain $SiO(OSi)_3$ units. These silicate species require tetraalkylammonium (TAA) ions for stabilization in both solution and the solid state and are destabilized by sodium ion in solution.[52]

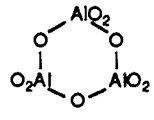

The number of possible linear oligomeric and polymeric chain aluminates is infinite,[58] even if one considers only straight chains containing $AlO_2(OAl)_2$ units (branched chains would require $AlO(OAl)_3$ units). The two simplest structural arrangements, denoted 1T and 2T, have structures of the type shown below in terms of successive $AlO_2(OAl)_2$ units, which are represented here in terms of AlO_4 tetrahedra drawn in perspective (assuming there is an aluminum atom at the center and an oxygen atom at each corner).

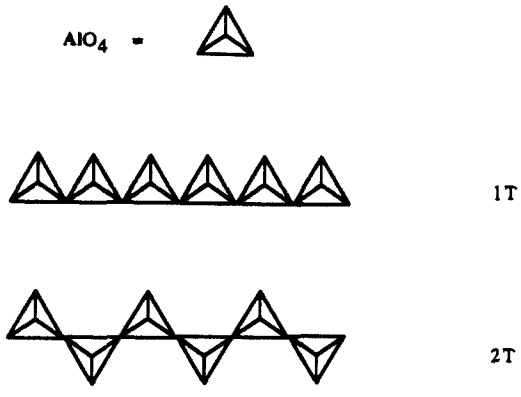

III

The solid-state ^{27}Al NMR evidence presented in this work is consistent with, but cannot distinguish among, aluminate structures such as the cyclic trimer (six-membered ring), the cyclic tetramer (eight-membered ring), as well as linear chains of variable length such as structure 2T. Aluminum in all of these structures has the local structure $AlO_2(OAl)_2$. However, a 2T-type structure for untreated $Na_2O·Al_2O_3·3H_2O$ is likely; the analogous aluminate systems, α-$Ba(AlO(OH)_2)_2$ and γ-$Ba(AlO(OH)_2)_2$, both contain linear chains formed by linking AlO_4 tetrahedra.[56,57] In both cases the chains of AlO_4 tetrahedra closely resemble a 2T-type structure. A global structure of the 2T-type for untreated $Na_2O·Al_2O_3·3H_2O$ leads to the conclusion that there is one non-structural water molecule in a formula unit of $Na_2O·Al_2O_3·3H_2O$.

For structural models based on either cyclic or linear chain aluminate structures, the presence of two different sodium sites of equal abundance observed in untreated $Na_2O·Al_2O_3·3H_2O$ must be accommodated. Three-dimensional models formed from parallel 2T chains of AlO_4 tetrahedra show that two different six-coordinate sodium sites may exist. One CN = 6 sodium site has six –OH nearest neighbors. The second CN = 6 sodium site has three –OH and two –OAl≤ nearest neighbors; the sixth nearest-neighbor oxygen atom may come from the nonstructural water molecule. It should be emphasized that these six-coordinate sodium sites are hypothetical sites and have only been pointed out as possibilities in order to show that at least two different six-coordinate sodium sites can be found in a global $Na_2O·Al_2O_3·3H_2O$ structure based on parallel, linear 2T-type chains; thus, a 2T-based aluminate structure is consistent with both the ^{23}Na and ^{27}Al NMR data reported in this work. The minor sodium component (peak B in the ^{23}Na NMR spectra) may be due to irregular, partially dehydrated sites of the sodium oxide type.

The ^{27}Al NMR spectrum of the dehydration product indicates that aluminum is in a highly symmetrical environment, i.e, the product consists of isolated AlO_4 tetrahedra with the sodium counterions symmetrically situated about aluminum in the tetrahedra. The major sodium ion component of the dehydration product fills the countercation role. The additional minor sodium component (peak E) may be due to inhomogeneous, partially dehydrated zones consisting of sodium sites of the sodium oxide type, formed during the synthesis of solid $Na_2O·Al_2O_3·3H_2O$ or during its dehydration at temperatures less than or equal to 600 °C.

Conclusions

^{23}Na and ^{27}Al NMR spectra obtained with use of high magnetic fields and high-speed MAS provide a powerful method for the structural investigation of $Na_2O·Al_2O_3·3H_2O$ and the chemical changes brought about by thermal dehydration. The spectral parameters yielded by NMR measurements of these non-integer quadrupolar nuclei permit various structures to be assigned to the chemically distinct sodium and aluminum sites present. The combination of ^{23}Na and ^{27}Al MAS NMR results provides useful insights into possible global structures of $Na_2O·Al_2O_3·3H_2O$ in various states of hydration. The assignments of ^{23}Na chemical shifts to specific structures is rendered difficult by the paucity of background NMR data; systematic ^{23}Na MAS NMR investigation of a wide variety of sodium compounds would be very useful for expanding background information for ^{23}Na structural assignments in complex solids.

Acknowledgment. We gratefully acknowledge partial support of this work by National Science Foundation Grants CHE-8610151 and RII-8902066, use of the Colorado State University Regional NMR Center, funded by National Science Foundation Grant No. CHE-8616437, and Hare Research, Inc. (Woodinville, WA) for donating the FTNMR software package to the Colorado State University Regional NMR Center. In addition, one of the authors (J.J.F.) acknowledges the support of the Alcoa Foundation.

Registry No. $Na_2O·Al_2O_3·3H_2O$, 51403-78-2.

(51) Englehardt, V. G.; Zeigan, D.; Jancke, H.; Hoebbel, D.; Wieker, W. *Z. Anorg. Allgr. Chem.* **1975**, *418*, 17-28.
(52) Lippmaa, E.; Magi, M.; Samoson, A.; Engelhardt, G.; Grimmer, A. R. *J. Am. Chem. Soc.* **1980**, *102*, 4889-4893.
(53) Engelhardt, G.; Randemacher, O. *J. Mol. Liquids* **1984**, *27*, 125-131.
(54) Harris, R. K.; Knight, C. T. G. *J. Chem. Soc., Faraday Trans. 2* **1983**, *79*, 1525-1538.
(55) Harris, R. K.; Knight, C. T. G. *J. Chem. Soc., Faraday Trans. 2* **1983**, *79*, 1539-1561.
(56) Ahmed, A. H. M.; Dent Glasser, L. S. *Acta Crystallogr.* **1970**, *B26*, 1686-1690.
(57) Dent Glasser, L. S.; Giovanoli, R. *Acta Crystallogr.* **1972**, *B28*, 760-763.
(58) Reference 44, pp 1009-1043.